New information on the early Permian lanthanosuchoid *Feeserpeton oklahomensis* based on Computed Tomography

Mark J. MacDougall [Corresp., 1] , **Anika Winge** [1] , **Jasper Ponstein** [1] , **Maren Jansen** [1, 2] , **Robert R. Reisz** [3] , **Jörg Fröbisch** [1, 4]

[1] Museum für Naturkunde Leibniz-Institute für Evolutions- und Biodiversitätsforschung, Berlin, Germany

[2] Museum für Naturkunde Magdeburg, Magdeburg, Germany

[3] University of Toronto Mississauga, Mississauga, Ontario, Canada

[4] Humboldt-Universität zu Berlin, Berlin, Germany

Corresponding Author: Mark J. MacDougall
Email address: mark.macdougall@mfn.berlin

The cave deposits of the Lower Permian Richards Spur locality in Oklahoma, USA, have produced an incredible number of terrestrial tetrapod taxa, many of which are currently only known from this locality. One of the many recent taxa to be described from the locality was the small lanthanosuchoid parareptile *Feeserpeton oklahomensis*. Represented by a well-preserved, near complete skull, *F. oklahomensis* would have been a small predatory reptile, likely preying upon arthropods, and contributes to the extensive tetrapod fauna that was present at Richards Spur. New computed tomography (CT) data of the holotype and only specimenhas allowed us to visualize and describe previously obscured and inaccessible anatomy of this taxon. These areas include the mandibular ramus, the palate, the sphenethmoid, the epipterygoids, and the braincase. Furthermore, this new anatomical information allowed formerly unknown character codings to be updated, thus we also performed new phylogenetic analyses that incorporated this new information. The results of these updated phylogenetic analyses are very similar to those of past studies, with *F. oklahomensis* being found as the sister taxon to all other lanthanosuchoids.

1 **New information on the early Permian lanthanosuchoid *Feeserpeton oklahomensis* based**
2 **on Computed Tomography**

4 Mark J. MacDougall [1], Anika Winge[1], Jasper Ponstein[1], Maren Jansen[1,2], Robert R. Reisz[3], and
5 Jörg Fröbisch[1,4]

7 [1]Museum für Naturkunde Leibniz-Institute für Evolutions- und Biodiversitätsforschung,
8 Invalidenstraße 43, 10115 Berlin, Germany
9 [2]Museum für Naturkunde Magdeburg, Otto-von-Guericke-Straße 68-73, 39104 Magdeburg,
10 Germany
11 [3]University of Toronto Mississauga, 3359 Mississauga Rd., Mississauga, Ontario, L5L1C6,
12 Canada
13 [4]Humboldt-Universität zu Berlin, Invalidenstraße 42, 10115 Berlin, Germany

15
16
17
18
19
20
21
22
23
24
25
26
27
28
29
30
31
32
33
34
35
36
37
38
39
40
41

42 Corresponding Author:
43 Mark MacDougall
44 Museum für Naturkunde Leibniz-Institute für Evolutions- und Biodiversitätsforschung,
45 Invalidenstraße 43, 10115 Berlin, Germany
46 Email address: mark.macdougall@mfn.berlin

47
48

49 **Abstract**
50
51 The cave deposits of the Lower Permian Richards Spur locality in Oklahoma, USA, have

52 produced an incredible number of terrestrial tetrapod taxa, many of which are currently only

53 known from this locality. One of the many recent taxa to be described from the locality was the

54 small lanthanosuchoid parareptile *Feeserpeton oklahomensis*. Represented by a well-preserved,

55 near complete skull, *F. oklahomensis* would have been a small predatory reptile, likely preying

56 upon arthropods, and contributes to the extensive tetrapod fauna that was present at Richards

57 Spur. New computed tomography (CT) data of the holotype and only specimen has allowed us to

58 visualize and describe previously obscured and inaccessible anatomy of this taxon. These areas

59 include the mandibular ramus, the palate, the sphenethmoid, the epipterygoids, and the braincase.

60 Furthermore, this new anatomical information allowed formerly unknown character codings to

61 be updated, thus we also performed new phylogenetic analyses that incorporated this new

62 information. The results of these updated phylogenetic analyses are very similar to those of past

63 studies, with *F. oklahomensis* being found as the sister taxon to all other lanthanosuchoids.

64

65

Introduction

66

67   The Lower Permian (Cisuralian) Richards Spur locality of southwestern Oklahoma,

68   represented by an extensive cave system, is known for its immense terrestrial tetrapod fauna

69   (Sullivan & Reisz, 1999; MacDougall et al., 2017b). Over the last few decades, more than 30

70   taxa have been described from the locality (MacDougall et al., 2017b), which includes various

71   anamniote tetrapods, synapsids, and reptiles. Among these tetrapods are numerous parareptile

72   taxa, specifically: *Colobomycter pholeter* Vaughn, 1958, *Delorhynchus priscus* Fox, 1962,

73   *Bolosaurus grandis* Reisz et al., 2002, *Microleter mckinzieorum* Tsuji et al., 2010, *Abyssomedon*

74   *williamsi* MacDougall and Reisz, 2014, *Delorhynchus cifelli* Reisz et al., 2014, and

75   *Colobomycter vaughni* MacDougall et al., 2016. Most early Permian continental assemblages

76   exhibit only a single parareptile taxon; Richards Spur is in stark contrast to this pattern, with

77   eight parareptiles being known from the locality (MacDougall et al., 2017b), several of which

78   belong to the clade Lanthanosuchoidea (Vaughn, 1958; Fox, 1962; Modesto, 1999; MacDougall

79   & Reisz, 2012; Reisz, MacDougall & Modesto, 2014; MacDougall, Modesto & Reisz, 2016).

80   Lanthanosuchoidea is a small clade of reptiles that includes various early and middle

81   Permian forms. Currently, all early Permian lanthanosuchoids are only known from North

82   America, whereas as the middle Permian taxa are known only from Russia. There are also

83   notable differences between the North American and Russian lanthanosuchoids. The early

84   Permian North American taxa are considered to be small, fully-terrestrial, predatory taxa

85   (Modesto, Scott & Reisz, 2009; Haridy, MacDougall & Reisz, 2017; MacDougall et al., 2017a),

86   whereas the middle Permian Russian taxa are larger and considered to be semi-aquatic

87   (Sennikov, 1996; Reisz, 1997; Verrière, Brocklehurst & Fröbisch, 2016). Overall, this suggests

88   that the clade could have potentially originated in western Laurasia and later dispersed to eastern

89   Laurasia, though the lack of Russian early Permian strata makes this biogeographic hypothesis

90   difficult to test.

91   The lanthanosuchoid *Feeserpeton oklahomensis* is one of the most recently described

92   taxa from Richards Spur locality and is currently only known from its holotype (MacDougall &

93   Reisz, 2012). It is represented by a small, nearly complete skull, and is characterized by several

94   enlarged maxillary teeth on the maxillae and dentaries, as well as large postorbitals and small

95   squamosals. In the initial description, MacDougall and Reisz (2012) largely described the visible

96   external anatomy of the skull, although CT data was used to examine the mandibular dentition.

97   However, they did not examine any other areas of the skull that were obscured or inaccessible,

98   which left some aspects of the anatomy of the skull unknown.

99   Herein, we describe the previously inaccessible anatomy of *Feeserpeton oklahomensis*

100   using new CT data. Areas that were segmented and examined include obscured parts of the lower

101   jaw and palate, the sphenethmoid, the epipterygoids, and elements of the braincase (Fig. 1).

102   Furthermore, the new information obtained from this data also warranted updating the

103   phylogenetic character codings of *F. oklahomensis*, thus updated phylogenetic analyses were

104   performed as well.

105

106   **Institutional Abbreviations: OMNH**, Sam Noble Oklahoma Museum of Natural History,

107   Norman, Oklahoma, USA.

108

109

110   **Materials & Methods**

111   **Specimen**

112   The skull of *Feeserpeton oklahomensis* examined for this study is the holotype and

113 currently only known specimen, OMNH 73541. It was previously studied and described by

114 MacDougall and Reisz (2012).

115

116 **Computed Tomography Data**

117   The skull of *Feeserpeton oklahomensis* was scanned using the x-ray computed

118 tomography setup (Phoenix | x-ray Nanotom | s) at the Museum für Naturkunde in Berlin. Scan

119 parameters were set to 57 kV voltage and 170µA current with 1440 images /360° at an exposure

120 time of 1000ms/image and an effective voxel size of 0.0129 mm, resulting in a magnification

121 rate of 3.857. Cone beam reconstruction was performed using datos | x-ray sensing 4 Inspection

122 Technologies GmbH (phoenix | x-ray) with a correction value of 1.845. The elements were

123 visualized and digitally segmented in VG studio Max 3.2. Smoothing of elements was

124 accomplished by rendering the images using the volume rendering setting 'Phong' with an

125 oversampling of 2.

126

127 **Phylogenetic Analyses**

128   The data matrix used in the two phylogenetic analyses is based on the data matrix of

129 MacDougall et al. (2018). The analyses were performed in PAUP 4.0a165 (Swofford, 2003),

130 using parsimony as the optimality criterion. The outgroup was set to include the taxa *Seymouria*,

131 *Limnoscelis*, and *Orobates*. Furthermore, minimum branch lengths of zero were set to collapse.

132 For the first analysis a heuristic search (TBR) was performed, with the addition sequence

133 algorithm set to simple, and multistate characters unordered. Both a bootstrap (1000 replicates)

134 and Bremer decay analysis were conducted to determine support values for clades.

135   We also performed a second analysis using the methodology documented by Laurin &

136   Piñeiro (2018) to see how the ordering of characters would affect tree topology and support

137   values.

138   The character codings of *Feeserpeton oklahomensis* were updated based on new

139   information obtained from the CT data. The characters that were recoded are as follows:

140   interpterygoid vacuity anterior extent (61) ?→0, alar flange of the vomer presence or absence

141   (64) ?→0, cultriform process present; (67) ?→1, pterygoid anterior extent (85) ?→0, cultriform

142   process anterior extent (86) ?→1, sutural contact between paroccipital process and

143   dermatocranium (92) ?→1, Meckelian fossa orientation (108) ?→0, Meckelian fossa

144   anteroposterior length (109) ?→0, number of coronoids (113) ?→1, prearticular anterior extent

145   (114) 1→0, coronoid process height (119) ?→0, high coronoid process composition (120) ?→-,

146   single large tooth on anteriormost end of vomer (169) 1→0. Furthermore, a few characters were

147   recoded for other taxa to correct some coding errors; these changes are indicated in the data

148   matrix. The updated data matrix and the full character list can be found in the supplementary

149   info.

150

151

152   **Description**

153   The CT data of *Feeserpeton oklahomensis* allowed for several previously inaccessible

154   and obscured areas of the skull to be examined and segmented (Fig. 1). These areas include parts

155   of the palate and the mandible, the sphenethmoid, the epipterygoids, and elements of the

156   braincase.

157

158   **The Palate**

159   Many of the palatal elements of *Feeserpeton oklahomensis* are visible in the holotype;

160   however, only the right side of the palate was prepared, and there are portions of it that are

161   obscured by supportive matrix. Through segmentation of the CT data both sides of the palate are

162   visible in their entirety (Fig. 2), some parts of the palate are damaged or not preserved, but it is

163   largely intact. The most notable feature of the palate that is clarified is the extent of the palatal

164   dentition, in particular on the palatine. The left palatine appears to be largely complete and grants

165   us a view of the element that was not available previously.

166   As was suggested by MacDougall and Reisz (2012), the palatine is a large element and

167   makes up a considerable portion of the overall palatal surface. Anteriorly, the palatine contacts

168   the vomer, whereas it contacts the pterygoid medially and posteriorly, the ectopterygoid is also

169   contacted posteriorly. Laterally, there is a contact with the maxilla. MacDougall and Reisz

170   (2012) note that there are two clusters of palatine teeth visible, though the full extent of these

171   clusters could not be fully determined. The segmented left palatine clearly shows that there is a

172   lateral and medial group of teeth on the element; they are roughly organized in the form of rows.

173   The lateral row consists of seven large teeth and a few smaller ones, whereas the medial row

174   consists of several smaller teeth.

175   The full anteroposterior extent of the vomer is also now apparent, the element is about the

176   same length as the palatine, and ends anteriorly with a narrow, pointed medially positioned

177   process. Likewise, the full lateral extent of the element reveals that the anterior end of the

178   palatine is nestled between two posterior extensions of the vomer: a broad medial extension, and

179   a narrower lateral one.

180   There are other features of the palate that are clarified with this new CT data. It is now

181   clear that the interpterygoid vacuity extends quite far anteriorly, past the posterior edge of the

182   palatines. Likewise, it is apparent that the cultriform process of the parasphenoid extends

183   forward for much of the length of the vacuity. Furthermore, the dorsal surface of the

184   parasphenoid is now visible for the first time, revealing several previously unknown aspects of

185   its anatomy. Anteriorly, where the cultriform process merges with the body of the parasphenoid,

186   a small pit, the sella turcica, is visible. Immediately posterior to this pit is the dorsum sellae, a

187   slightly raised wall that borders the sella turcica. Unfortunately, due to the poorer resolution of

188   the CT data in this area, certain features of the parasphenoid were not able to be segmented,

189   specifically the small teeth that are present on this element (MacDougall & Reisz, 2012).

190   Furthermore, a suborbital foramen is not present, with the palate being unbroken at the

191   intersection of the pterygoid, palatine, and ectopterygoid, as is the case in other lanthanosuchoids

192   (deBraga & Reisz, 1996; Reisz, MacDougall & Modesto, 2014).

193

194   **The Mandible**

195   Due to the mandibular rami of *Feeserpeton oklahomensis* being occluded with the upper

196   jaw, only details of the ventral and labial surfaces can be clearly observed, with much of the

197   dorsal and lingual surfaces being obscured by the occlusion. However, segmentation of the entire

198   left mandibular ramus (Fig. 3) reveals new information regarding these previously inaccessible

199   areas. The left ramus is slightly damaged on its labial surface, which results in a small gap

200   through which the labial surface of the prearticular can be seen.

201   MacDougall and Reisz (2012) used CT data to investigate the dentition of the dentary,

202   though only the shape of the teeth was examined. The segmented mandibular ramus of the

203   holotype exhibits 21 teeth on the dentary, however, when empty alveoli are included the total

204   number of dentary teeth increases to 25. Furthermore, there are enlarged teeth found on the

205   anterior end of the element; there are two visible and an empty alveolus, suggesting that there

206   would have been three enlarged teeth, the same pattern that is observed on the maxilla

207   (MacDougall & Reisz, 2012).

208   One of the more notable features of the mandible are the coronoid elements (Figs. 3, 4).

209   In their investigation of multiple coronoids and coronoid dentition in Palaeozoic reptiles, the

210   coronoid of *Feeserpeton oklahomensis* was examined by Haridy et al. (2017) using CT data.

211   They identified the presence of two coronoids on each ramus, as well as the presence of coronoid

212   dentition. We are able to confirm that coronoid dentition is present in *F. oklahomensis* (Fig. 4),

213   though much of the dentition appears to not be preserved, there are three small teeth that are

214   clearly visible on the right coronoid. However, unlike what was observed by Haridy et al. (2017),

215   we find no trace of two coronoid elements (Fig. 3), suggesting that the presence of multiple

216   coronoids in *F. oklahomensis* was likely a misinterpretation.

217   The coronoid itself is a relatively long element found lingual to the posterior end of the

218   dentary. It extends anteriorly from its posterior articulation with the surangular to the 18th tooth

219   position of the dentary, narrowing for most of its length. A posteroventral process of the

220   coronoid curves posteriorly to meet with the prearticular.

221   The splenial is largely restricted to the medial surface of the mandibular ramus (Fig. 3),

222   making it difficult to examine fully previously. Anteriorly, the two splenials would have met

223   with another and contributed to the mandibular symphysis. The anterior end of the splenial also

224   exhibits the presence of the foramen intermandibularis oralis. Usually, in early reptiles there was

225   also a foramen intermandibularis caudalis found at the intersection of the splenial, angular, and

226   prearticular, but it does not appear to be present in this specimen of *F. oklahomensis*, which may

227   be the result of the slight damage present in this area.

228   The full extent of the prearticular, an element not described by MacDougall and Reisz

229   (2012), is revealed in the segmented mandibular ramus (Fig. 3). It is a long element that extends

230   from the articular to the posterior end of the splenial. It also articulates ventrally with the portion

231   of the angular that wraps around to the medial side of the ramus, whereas its anterodorsal edge

232   contacts the coronoid and dentary. The dorsal portion of the prearticular forms the medial margin

233   of the large adductor fossa. Overall, the prearticular is quite similar in shape and position to that

234   of other closely related taxa, such as *Delorhynchus* (Haridy, MacDougall & Reisz, 2017).

235   The Meckelian fossa, normally completely obscured by the occlusion of the jaws to the

236   rest of the skull, is revealed in its entirety in the segmented mandibular ramus as well (Fig. 3).

237   The Meckelian fossa of *Feeserpeton oklahomensis* is found on the posterior end of the

238   mandibular ramus. The fossa faces dorsomedially and it is quite long, extending anteriorly for

239   about a third of the length of the ramus, as is the case in *Delorhynchus* (Haridy, MacDougall &

240   Reisz, 2017).

241

242   **The Sphenethmoid**

243   The sphenethmoid is a rarely described element in early reptiles, usually because it is

244   either not preserved or not visible. Due to the internal position of the sphenethmoid in the

245   holotype of *Feeserpeton* it was not noted or discussed in MacDougall and Reisz (2012), here we

246   present the fully segmented sphenethmoid element (Fig. 5).

247   The sphenethmoid is found in its expected position, ventral to the frontals. It is a roughly

248   Y-shaped element when viewed in anterior and posterior aspects, possessing a slender ventral

249   process (often termed the keel) and two equally slender dorsal processes with a rounded trough

250   between them. Lateral view of the element reveals that its anteroposterior length is about

251   equivalent to its dorsoventral height. This sphenethmoid shape is similar to what has been

252   observed in other early reptiles, such as *Captorhinus* (Heaton, 1979; Modesto & Reisz, 2008).

253

254   **The Epipterygoids**

255   The epipterygoids are another example of rarely described elements of early reptiles,

256   largely due to their interior position within the skull. The new CT data reveal the presence of

257   both epipterygoids in the holotype of *Feeserpeton oklahomensis*, which were both fully

258   segmented for the purpose of this study (Fig. 6). These elements were not described by

259   MacDougall and Reisz (2012) as they are not exposed externally. Both epipterygoids appear to

260   be disarticulated and not in their natural positions (Fig. 1), but overall they are similar in

261   structure to those that have been described for other early reptiles (Romer, 1956; Carroll &

262   Lindsay, 1985), possessing a gracile dorsal columella that arches slightly posterior, and a ventral

263   region that expands to form a more robust footplate with a broad anteroposterior length. The

264   footplate also exhibits a process on its anteromedial surface, a characteristic that has also been

265   observed in other early reptiles, such as *Captorhinus* (Fox & Bowman, 1966). In their natural

266   positions the dorsal columella of each epipterygoid would have contacted the supraoccipital and

267   prootic, whereas the footplate would have presumably met with the quadrate process of the

268   pterygoid, as is the case in *Captorhinus* (Fox & Bowman, 1966) and the procolophonids

269   *Leptopleuron* and *Hypsognathus* (Sues et al., 2000; Cisneros, 2008).

270

271   **The Braincase**

272   The braincase of *Feeserpeton oklahomensis* was described externally by MacDougall and

273   Reisz (2012), however, there was still substantial portions of its overall anatomy that could not

274   be described due to being obscured. The fully segmented braincase presented here (Fig. 7)

275   reveals several details that could not be observed in the original description of the holotype. It is

276   also quite apparent that the braincase exhibits slight disarticulation of elements from their natural

277   position, as well as some damaged areas.

278   The prootics of *Feeserpeton* are large, irregularly shaped anterior elements of the

279   braincase and form an extensive portion of its overall structure. While MacDougall and Reisz

280   (2012) were able to identify the prootics, they were only able to describe the exposed ventral

281   surface of the elements, which is only a small portion of the overall element. The prootics appear

282   to be entirely intact but are slightly disarticulated and not in contact with most of the other

283   elements of the braincase, though laterally they do have a slight contact with their respective

284   opisthotics. The posterior surface of the prootic would have articulated with the anterior surface

285   of the opisthotic. The flattened posterolateral extension of the element, usually termed the

286   paroccipital process of the prootic would have met with the paroccipital process of the opisthotic,

287   with a large depression in this region of the prootic contributing to the fenestra ovalis.

288   Dorsomedially, there is a small process that would have met with the supraoccipital. The medial

289   portion of the element exhibits another smaller process that extends ventrally out from the main

290   body of the prootic, which would likely have come close to contacting the basioccipital. The

291   anterior part of the prootic is convex in shape. Overall, the structure of the prootic is largely

292   similar to what has been described for other parareptiles, such as *Leptopleuron* (Spencer, 2000),

293   though in the case of *Leptopleuron* the prootic appears to be not quite as robust as that of

294   *Feeserpeton*. Unfortunately, this is a rarely described element of closely related taxa, due to its

295   often-inaccessible position.

296   The opisthotics are another large component of the braincase, and like the prootics, they

297   were also only partially described by MacDougall and Reisz (2012). The segmented braincase

298   clearly illustrates that both of the opisthotics suffer from damage (Fig. 7), however, the left

299   opisthotic is substantially more damaged than the right one, with a large posterior segment of the

300   element being completely absent. The better preserved right opisthotic clearly exhibits a laterally

301   expanded anterodorsal end, and a posterior portion that extends ventrally. The broad anterior end

302   contributes to the paroccipital process of the opisthotic, which would have met with the

303   paroccipital process of the prootics. Moving medially the posterior portion of the opisthotic

304   expands dorsoventrally and meets with the lateral edge of the fused exoccipital-basioccipital

305   complex, contributing to the posterior end of the braincase and forming the remaining portion of

306   the paroccipital process.

307   The stapes was briefly described by (MacDougall & Reisz, 2012), and we expand upon

308   their description here. The stapes of *Feeserpeton* is not in its natural position, being slightly

309   disarticulated; it consists of a bifurcating laterally compressed distal end, and the broad

310   proximally located footplate, which are connected by a short, slightly twisted shaft. In its natural

311   position the footplate would have met with the fenestra ovalis of the paraoccipital process, with

312   the distal end extending laterally towards the quadrate. The distal end of the stapes bifurcates

313   into two distinct processes, the distal facing columella, which appears to be broken, and prior to

314   this process a dorsal extension. The stapes is similar in size and structure to the stapes of

315   *Acleistorhinus pteroticus* (deBraga & Reisz, 1996), but is quite distinct from the small gracile

316   stapes of *Leptopleuron lacertinum* (Spencer, 2000).

317

318

Phylogenetic Analyses

320   The first phylogenetic analysis produced 27 optimal trees, each with a tree length of 667.

321 As in the original MacDougall and Reisz (2012) study, the strict consensus tree (Fig. 8) produced

322 from the optimal trees has *Feeserpeton oklahomensis* being recovered as the sister taxon of all

323 other lanthanosuchoids (it is in this position in all 27 of the optimal trees). The clade

324 Lanthanosuchoidea is recovered as the sister taxon to the clade that contains Bolosauria,

325 Procolophonoidea, Pareiasauridae, Nycteroleteridae, Nyctiphruretidae, and *Microleter*. This is

326 similar to what was recovered in the analysis of MacDougall and Reisz (2012), except for the

327 inclusion of *Microleter* within this clade. However, the position of Bolosauria in our analysis

328 differs from what was recovered by other studies (Modesto et al., 2015; MacDougall et al.,

329 2017a), where the clade was found to be more basal than Lanthanosuchoidea.

330   Similar to the results of MacDougall et al. (2018), the ophiacodontid (*Archaeothyris*) and

331 varanopid taxa (*Archaeovenator, Mycterosaurus*) included in the analysis were recovered as

332 being more closely related to the reptile taxa than to the synapsids. This is an atypical result that

333 warrants further investigation in the future, but is at least partly in line with the results of recent

334 work that has recovered varanopids within Reptilia (Ford & Benson, 2018). In the case of our

335 study this result could potentially be the result of the relatively narrow focus of our analysis.

336   The second analysis in which characters were ordered following the methodology of

337 Laurin & Piñeiro (2018) produced 9 optimal trees, the consensus of which resulted in a very

338 similar tree (Fig. S1) to that recovered in our first analysis. The only difference being the

339   resolution of the polytomy that contained the nyctiphruretids, procolophonoids, pareiasaurs, and

340   nycteroleters.

341

Discussion

New Information from CT Data

344   The early Permian Richards Spur locality has produced a considerable amount of well-

345   preserved fossil material, largely due to the unique preservational environment associated with

346   the caves found there (MacDougall et al., 2017b). In particular near complete skulls are not

347   uncommon at the locality, with many taxa being known almost solely from skulls (e.g. Modesto

348   and Reisz, 2008; Anderson et al., 2009; Tsuji et al., 2010; Polley and Reisz, 2011; MacDougall

349   et al., 2017b). These various well-preserved specimens provide substantial information regarding

350   the anatomy of the taxa to which they belong, however, there are also various regions of these

351   skulls that cannot be examined normally, either due to being obscured or not being exposed

352   externally. CT data are proving to be an ideal way to study these skulls and their difficult to

353   examine areas, which will in turn provide more information regarding the Richards Spur

354   assemblage and the taxa that compose it. The new CT data of the holotype of *Feeserpeton*

355   *oklahomensis* have allowed for the segmentation of several previously inaccessible areas,

356   revealing more details regarding the anatomy of this taxon. Specifically, the dentition of the

357   mandible and palate, and various elements of the skull that are largely internal.

358   Recently, there have been other parareptile taxa that have been examined using CT data

359   (Tsuji, Sobral & Müller, 2013; Zaher, Coram & Benton, 2018), which resulted in the discovery

360   of new information about the examined taxa, however, there are still numerous parareptile taxa

361   that have yet to be examined in comparable detail using CT scanning. The new information that

362   will be obtained from examining other parareptiles using CT scans will be important for

363   resolving issues and testing existing hypotheses regarding early amniote relationships (Laurin &

364   Piñeiro, 2017, 2018; Ford & Benson, 2018; MacDougall et al., 2018), as well as for better

365   understanding the anatomy and evolution of these taxa (Zaher, Coram & Benton, 2018).

366

367   **The Coronoid Eminence of *Feeserpeton***

368   One of the aspects of the anatomy of *Feeserpeton oklahomensis* that was clarified with

369   CT data is the composition of the coronoid eminence. The coronoid eminence of

370   lanthanosuchoids has been shown to be quite complex, with the presence of multiple coronoids

371   and dentition present on the elements (Haridy, MacDougall & Reisz, 2017; MacDougall et al.,

372   2017a). Our identification of a single coronoid on the mandibular ramus of *F. oklahomensis* (Fig.

373   3), which is contrary to the observations of Haridy et al. (2017), does not dramatically change

374   their interpretations about the evolution of the trait within Lanthanosuchoidea. The only potential

375   change this reinterpretation introduces to their hypothesis is that the presence of multiple

376   coronoids does not appear to be primitive for Lanthanosuchoidea, instead appearing later in the

377   evolution of the clade. However, we were able to confirm that the coronoid of *F. oklahomensis*

378   does indeed exhibit dentition (Fig. 4), thus it is clear that denticulate coronoids are the primitive

379   condition for lanthanosuchoids, as was hypothesized by Haridy et al. (2017). Other

380   lanthanosuchoid taxa, notably *Acleistorhinus pteroticus*, will have to be reexamined in the future

381   to further elucidate details regarding the evolution of multiple and denticulate coronoids within

382   the clade.

383

384

385 **Conclusions**

386   Through computed tomography data and modern visualization techniques this study

387 reveals new information regarding the anatomy of the early Permian reptile *Feeserpeton*

388 *oklahomensis*. Notably, we were able to describe numerous details regarding the anatomy of the

389 mandibular rami, the palate, the sphenethmoid, the epipterygoids, and the braincase. All of which

390 are parts of the skull that cannot be fully examined normally in the holotype specimen. This new

391 information also allowed for several previously unknown phylogenetic characters to be coded.

392 The evolution and relationships of early amniotes is still an area of palaeontological research that

393 is far from set in stone, and the investigation of normally inaccessible anatomy using CT data has

394 been and will continue to be important for better understanding reptile, and more broadly, early

395 tetrapod evolution.

396

397

398 **Acknowledgements**

399   We would like to thank the Richard Cifelli and William May, for their assistance in

400 acquiring this and other specimens, we also thank Mike Feese for his assistance, and his donating

401 of many Richards Spur specimens to the OMNH. We also thank Sean Modesto, Michel Laurin,

402 and Juan Cisneros for reviewing the manuscript and providing very helpful comments. Mark J.

403 MacDougall was supported by a Leibniz-DAAD postdoctoral scholarship and currently a

404 Humboldt postdoctoral fellowship, Jasper Ponstein is supported by a Research Track Scholarship

405 of the Humboldt-Universität zu Berlin within the Excellence initiative of the states and the

406 federal government, Robert R. Reisz is supported by a National Science and Engineering

407 Research Council (NSERC) Discovery grant, and Jörg Fröbisch is supported by the German

408 Research Foundation (DFG).

409

410

References

412 Anderson JS, Scott D, Reisz RR. 2009. *Nannaroter mckinziei*, a new ostodolepid 'microsaur'

413   (Tetrapoda, Lepospondyli, Recumbirostra) from the Early Permian of Richards Spur

414   (Ft. Sill), Oklahoma. *Journal of Vertebrate Paleontology* 29:379–388. DOI:

415   10.1671/039.029.0222.

416 Carroll RL, Lindsay W. 1985. Cranial anatomy of the primitive reptile *Procolophon*.

417   *Canadian Journal of Earth Sciences* 22:1571–1587. DOI: 10.1139/e85-166.

418 Cisneros JC. 2008. Phylogenetic relationships of procolophonid parareptiles with remarks

419   on their geological record. *Journal of Systematic Palaeontology* 6:345–366. DOI:

420   10.1017/S1477201907002350.

421 deBraga M, Reisz RR. 1996. The Early Permian reptile *Acleistorhinus pteroticus* and its

422   phylogenetic position. *Journal of Vertebrate Paleontology* 16:384–395. DOI:

423   10.1080/02724634.1996.10011328.

424 Ford DP, Benson RBJ. 2018. A redescription of *Orovenator mayorum* (Sauropsida, Diapsida)

425   using high-resolution μCT, and the consequences for early amniote phylogeny.

426   *Palaeontology*.

427 Fox RC. 1962. Two new pelycosaurs from the Lower Permian of Oklahoma. *University of*

428   *Kansas Publications of the Museum of Natural History* 12:297–307.

429   Fox RC, Bowman MC. 1966. Osteology and relationships of *Captorhinus aguti* (Cope)

430   (Reptilia: Captorhinomorpha). *The University of Kansas Paleontological*

431   *Contributions* 11:1–79.

432   Haridy Y, MacDougall MJ, Reisz RR. 2017. The lower jaw of the Early Permian parareptile

433   *Delorhynchus*, first evidence of multiple denticulate coronoids in a reptile. *Zoological*

434   *Journal of the Linnean Society*. DOI: 10.1093/zoolinnean/zlx085.

435   Heaton MJ. 1979. Cranial anatomy of primitive captorhinid reptiles from the Late

436   Pennsylvanian and Early Permian, Oklahoma and Texas. *Oklahoma Geological Survey*

437   *Circular* 127:84.

438   Laurin M, Piñeiro GH. 2017. A reassessment of the taxonomic position of mesosaurs, and a

439   surprising phylogeny of early amniotes. *Frontiers in Earth Science* 5. DOI:

440   10.3389/feart.2017.00088.

441   Laurin M, Piñeiro G. 2018. Response: commentary: a reassessment of the taxonomic

442   position of mesosaurs, and a surprising phylogeny of early amniotes. *Frontiers in*

443   *Earth Science* 6. DOI: 10.3389/feart.2018.00220.

444   MacDougall MJ, Modesto SP, Brocklehurst N, Verrière A, Reisz RR, Fröbisch J. 2018.

445   Commentary: a reassessment of the taxonomic position of mesosaurs, and a

446   surprising phylogeny of early amniotes. *Frontiers in Earth Science* 6. DOI:

447   10.3389/feart.2018.00099.

448   MacDougall MJ, Modesto SP, Reisz RR. 2016. A new reptile from the Richards Spur locality,

449   Oklahoma, U.S.A., and patterns of Early Permian parareptile diversification. *Journal*

450   *of Vertebrate Paleontology* 36:e1179641. DOI: 10.1080/02724634.2016.1179641.

451   MacDougall MJ, Reisz R. 2012. A new parareptile (Parareptilia, Lanthanosuchoidea) from

452   the Early Permian of Oklahoma. *Journal of Vertebrate Paleontology* 32:1018–1026.

453   DOI: 10.1080/02724634.2012.679757.

454   MacDougall MJ, Reisz RR. 2014. The first record of a nyctiphruretid parareptile from the

455   Early Permian of North America, with a discussion of parareptilian temporal

456   fenestration. *Zoological Journal of the Linnean Society* 172:616–630. DOI:

457   10.1111/zoj.12180.

458   MacDougall MJ, Scott D, Modesto SP, Williams SA, Reisz RR. 2017a. New material of the

459   reptile *Colobomycter pholeter* (Parareptilia: Lanthanosuchoidea) and the diversity of

460   reptiles during the Early Permian (Cisuralian). *Zoological Journal of the Linnean*

461   *Society* 180:661–671. DOI: 10.1093/zoolinnean/zlw012.

462   MacDougall MJ, Tabor NJ, Woodhead J, Daoust AR, Reisz RR. 2017b. The unique

463   preservational environment of the Early Permian (Cisuralian) fossiliferous cave

464   deposits of the Richards Spur locality, Oklahoma. *Palaeogeography,*

465   *Palaeoclimatology, Palaeoecology* 475:1–11.

466   Modesto SP. 1999. *Colobomycter pholeter* from the Lower Permian of Oklahoma: a

467   parareptile, not a protorothyridid. *Journal of Vertebrate Paleontology* 19:466–472.

468   DOI: 10.1080/02724634.1999.10011159.

469   Modesto SP, Reisz RR. 2008. New material of *Colobomycter pholeter*, a small parareptile

470   from the Lower Permian of Oklahoma. *Journal of Vertebrate Paleontology* 28:677–

471   684. DOI: 10.1671/0272-4634(2008)28[677:NMOCPA]2.0.CO;2.

472   Modesto SP, Scott DM, MacDougall MJ, Sues H-D, Evans DC, Reisz RR. 2015. The oldest

473   parareptile and the early diversification of reptiles. *Proceedings of the Royal Society*

474   *of London B: Biological Sciences* 282:20141912. DOI: 10.1098/rspb.2014.1912.

475   Modesto SP, Scott DM, Reisz RR. 2009. Arthropod remains in the oral cavities of fossil

476   reptiles support inference of early insectivory. *Biology Letters* 5:838–840. DOI:

477   10.1098/rsbl.2009.0326.

478   Polley BP, Reisz RR. 2011. A new Lower Permian trematopid (Temnospondyli:

479   Dissorophoidea) from Richards Spur, Oklahoma. *Zoological Journal of the Linnean*

480   *Society* 161:789–815. DOI: 10.1111/j.1096-3642.2010.00668.x.

481   Reisz RR. 1997. The origin and early evolutionary history of amniotes. *Trends in Ecology &*

482   *Evolution* 12:218–222. DOI: 10.1016/S0169-5347(97)01060-4.

483   Reisz RR, Barkas V, Scott D. 2002. A new early Permian bolosaurid reptile from the

484   Richards Spur Dolese Brothers Quarry, near Fort Sill, Oklahoma. *Journal of*

485   *Vertebrate Paleontology* 22:23–28. DOI: 10.1671/0272-

486   4634(2002)022[0023:ANEPBR]2.0.CO;2.

487   Reisz RR, MacDougall MJ, Modesto SP. 2014. A new species of the parareptile genus

488   *Delorhynchus*, based on articulated skeletal remains from Richards Spur, Lower

489   Permian of Oklahoma. *Journal of Vertebrate Paleontology* 34:1033–1043. DOI:

490   10.1080/02724634.2013.829844.

491   Romer AS. 1956. *Osteology of the Reptiles*. Chicago: The University of Chicago Press.

492   Sennikov AG. 1996. Evolution of the Permian and Triassic tetrapod communities of Eastern

493   Europe. *Palaeogeography, Palaeoclimatology, Palaeoecology* 120:331–351. DOI:

494   10.1016/0031-0182(95)00041-0.

495   Spencer PS. 2000. The braincase structure of *Leptopleuron lacertinum* Owen (Parareptilia:

496   Procolophonidae). *Journal of Vertebrate Paleontology* 20:21–30. DOI:

497   10.1671/0272-4634(2000)020[0021:TBSOLL]2.0.CO;2.

498   Sues H-D, Olsen PE, Scott DM, Spencer PS. 2000. Cranial osteology of *Hypsognathus fenneri*,

499   a latest Triassic procolophonid reptile from the Newark Supergroup of eastern

500   North America. *Journal of Vertebrate Paleontology* 20:275–284. DOI: 10.1671/0272-

501   4634(2000)020[0275:COOHFA]2.0.CO;2.

502   Sullivan C, Reisz RR. 1999. First record of *Seymouria* (Vertebrata: Seymouriamorpha) from

503   Early Permian fissure fills at Richards Spur, Oklahoma. *Canadian Journal of Earth*

504   *Sciences* 36:1257–1266. DOI: 10.1139/e99-035.

505   Swofford DL. 2003. *PAUP*. Phylogentic Analysis Using Parsimony (*and Other Methods).*

506   Sunderland, Massachusetts: Sinauer Associates.

507   Tsuji LA, Müller J, Reisz RR. 2010. *Microleter mckinzieorum* gen. et sp. nov. from the Lower

508   Permian of Oklahoma: the basalmost parareptile from Laurasia. *Journal of*

509   *Systematic Palaeontology* 8:245–255. DOI: 10.1080/14772010903461099.

510   Tsuji LA, Sobral G, Müller J. 2013. *Ruhuhuaria reiszi*, a new procolophonoid reptile from the

511   Triassic Basin of Tanzania. *Comptes Rendus Palevol* 12:487-494.

512   Vaughn PP. 1958. On a new pelycosaur from the lower Permian of Oklahoma, and on the

513   origin of the family Caseidae. *Journal of Paleontology* 32:981–991.

514   Verrière A, Brocklehurst N, Fröbisch J. 2016. Assessing the completeness of the fossil

515   record: comparison of different methods applied to parareptilian tetrapods

516   (Vertebrata: Sauropsida). *Paleobiology* 42:680–695. DOI: 10.1017/pab.2016.26.

517 Zaher M, Coram RA, Benton MJ. 2018. The Middle Triassic procolophonid *Kapes bentoni*:

518   computed tomography of the skull and skeleton. *Papers in Palaeontology* 5:111–138.

519   DOI: 10.1002/spp2.1232.

520

521

Figure Captions

523 Figure 1. The skull of *Feeserpeton oklahomensis*, OMNH 73541, showing the regions that were

524 reconstructed using CT data. Scale bar equals 2 mm. [Half page width]

525

526 Figure 2. The palate of *Feeserpeton oklahomensis*, OMNH 73541, reconstructed from CT data.

527 **A**, dorsal view, and **B**, ventral view. Abbreviations: **ec**, ectopterygoid; **m**, maxilla; **pal**, palatine;

528 **ps**, parasphenoid; **pt**, pterygoid; **v**, vomer. Scale bar equals 4 mm. [Half page width]

529

530 Figure 3. The left mandibular ramus of *Feeserpeton oklahomensis*, OMNH 73541, reconstructed

531 from CT data. **A**, dorsal view, **B**, ventral view, **C**, labial view, and **D**, lingual view.

532 Abbreviations: **an**, angular; **ar**, articular; **c**, coronoid; **d**, dentary; **pra**, prearticular; **sa**,

533 surangular; **sp**, splenial. Scale bar equals 2 mm. [Half page width]

534

535 Figure 4. The right coronoid of *Feeserpeton oklahomensis*, OMNH 73541, reconstructed from

536 CT data. **A**, lingual view, and **B**, dorsal view. Scale bar equals 1 mm. [Half page width]

537

538 Figure 5. The sphenethmoid of *Feeserpeton oklahomensis*, OMNH 73541, reconstructed from

539 CT data. **A**, anterior view, **B**, posterior view, **C**, dorsal view, and **D**, right lateral view. Scale bar

540 equals 1 mm. [Half page width]

541

542 Figure 6. The left epipterygoid of *Feeserpeton oklahomensis*, OMNH 73541, reconstructed from

543 CT data. **A**, lateral view, **B**, medial view, **C**, dorsal view, and **D**, ventral view. Scale bar equals 1

544 mm. [Half page width]

545

546 Figure 7. The braincase of *Feeserpeton oklahomensis*, OMNH 73541, reconstructed from CT

547 data. **A**, dorsal view, **B**, ventral view, **C**, right lateral view, and **D**, posterior view. Abbreviations:

548 **bo**, basioccipital; **eo**, exoccipitals; **op**, opisthotic; **pro**, prootic; **ps**, parasphenoid; **so**,

549 supraoccipital; **st**, stapes; **?**, unknown fragment that may be part of the left stapes or the left

550 opisthotic. Scale bar equals 2 mm. [Half page width]

551

552 Figure 8. Strict consensus tree obtained from the first phylogenetic analysis, where characters

553 were unordered. Tree length =667, consistency index = 0.301, rescaled consistency index =

554 0.195, retention index = 0.647. Nodes of clades of interest are labeled: **A**, Amniota; **B**, Reptilia;

555 **C**, Parareptilia; **D**, Eureptilia; **E**, Lanthanosuchoidea; **F**, Bolosauria; **G**, Nyctiphruretidae; **H**,

556 Nycteroleteridae; **I**, Pareiasauridae; **J**, Procolophonoidea. Bootstrap support values are found

557 above nodes, if no value is indicated it was less than 50%. Bremer support values are found

558 below nodes, if no value is indicated the clade collapsed with the addition of one extra step.

559 [Half page width]

Figure 1

The skull of *Feeserpeton oklahomensis*, OMNH 73541,showing the regions that were reconstructed using CT data.

Scale bar equals 2 mm.

Figure 2

The palate of *Feeserpeton oklahomensis*, OMNH 73541, reconstructed from CT data.

A, dorsal view, and **B**, ventral view. Abbreviations: **ec**, ectopterygoid; **m**, maxilla; **pal**, palatine; **ps**, parasphenoid; **pt**, pterygoid; **v**, vomer. Scale bar equals 4 mm.
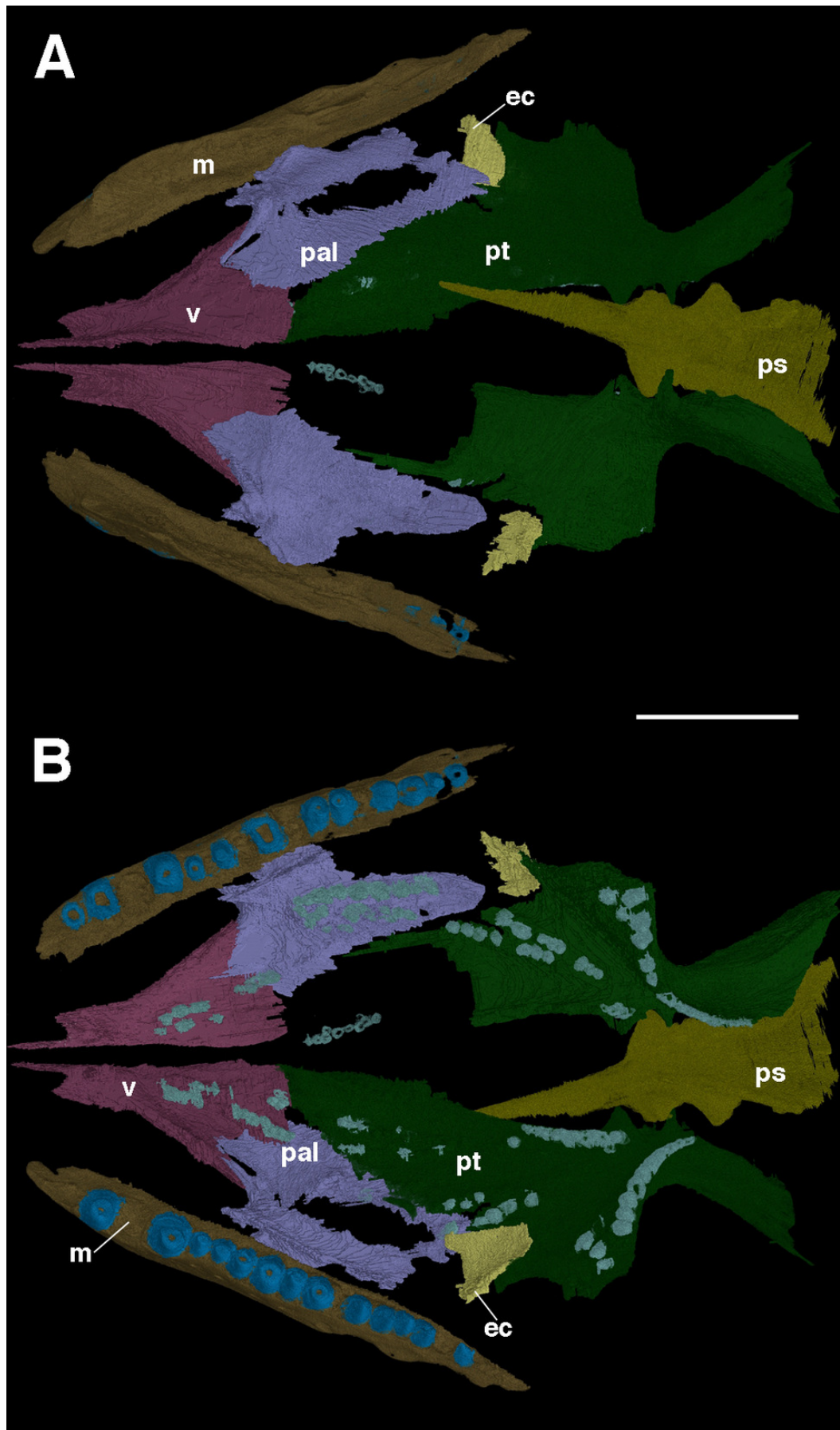
Figure 3

The left mandibular ramus of *Feeserpeton oklahomensis*, OMNH 73541,reconstructed from CT data.

A, dorsal view, **B**, ventral view, **C**, labial view, and**D**, lingual view. Abbreviations: **an**, angular; **ar**, articular; **c**, coronoid;**d**, dentary; **pra**, prearticular; **sa**, surangular;**sp**, splenial. Scale bar equals 2 mm.
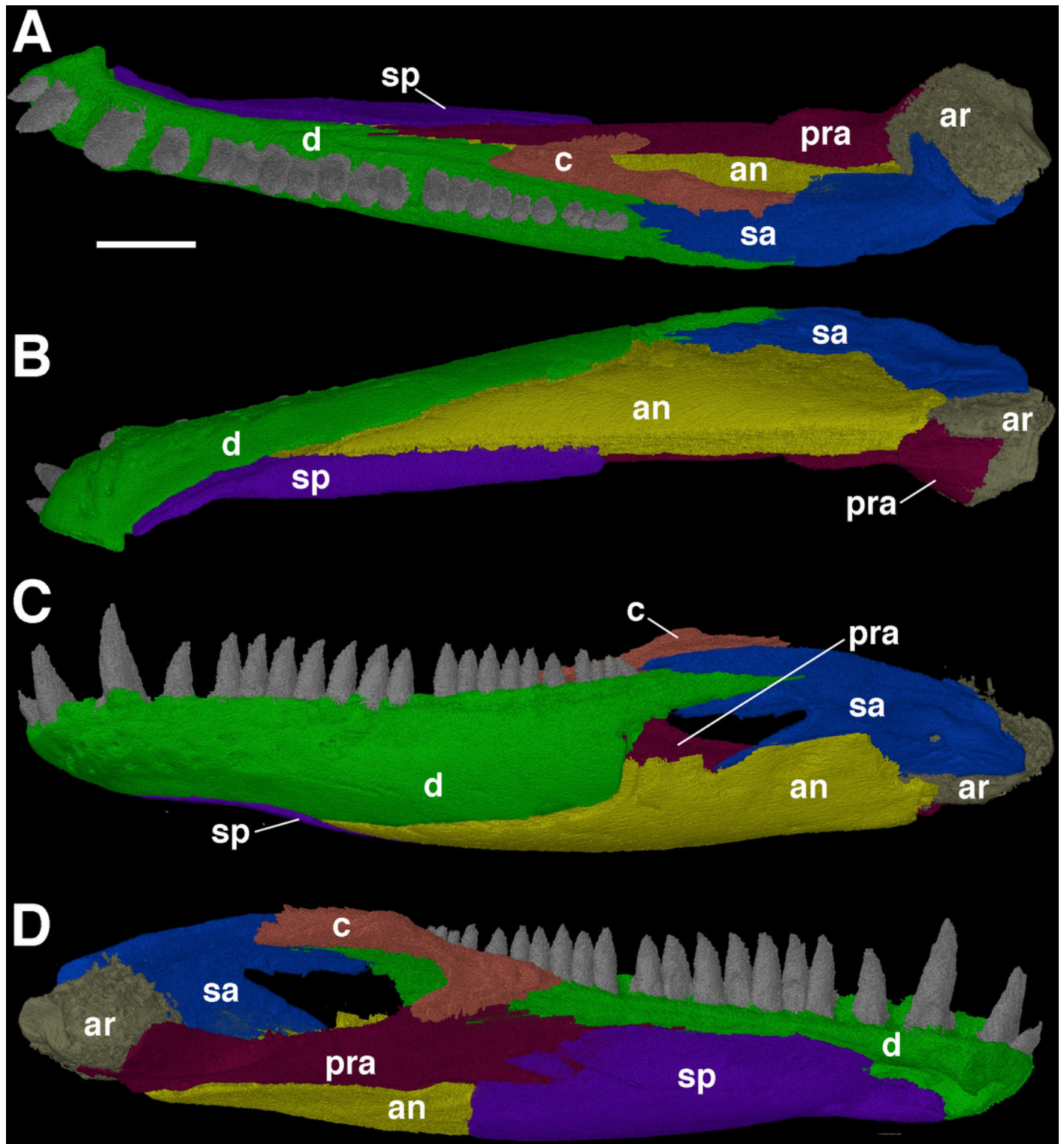
Figure 4

The right coronoid of *Feeserpeton oklahomensis*, OMNH 73541, reconstructed from CT data.

A, lingual view, and **B**, dorsal view. Scale bar equals 1 mm.
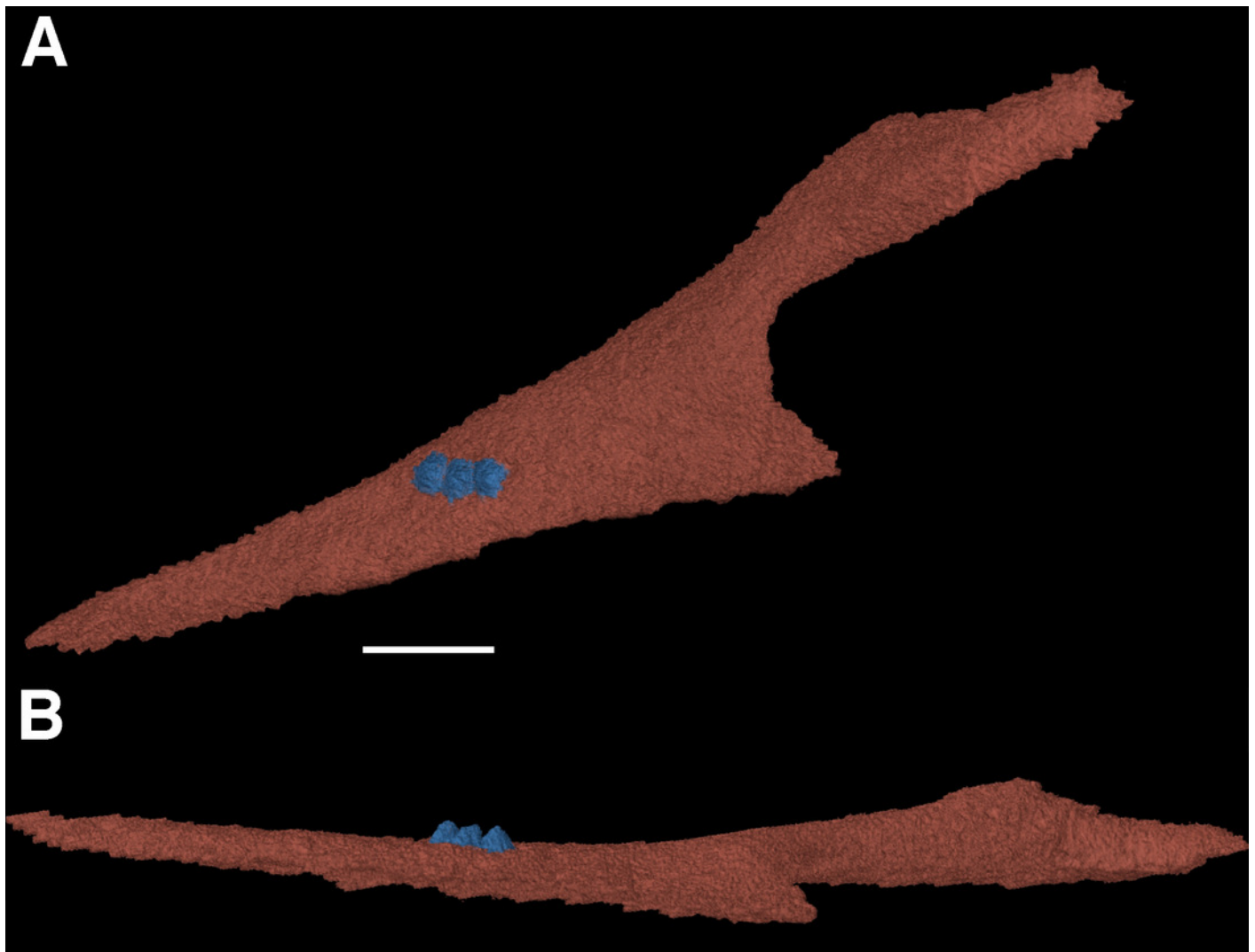
Figure 5

The sphenethmoid of *Feeserpeton oklahomensis*, OMNH 7354, reconstructed from CT data.

A, anterior view, **B**, posterior view, **C**, dorsal view, and **D**, right lateral view. Scale bar equals 1 mm.
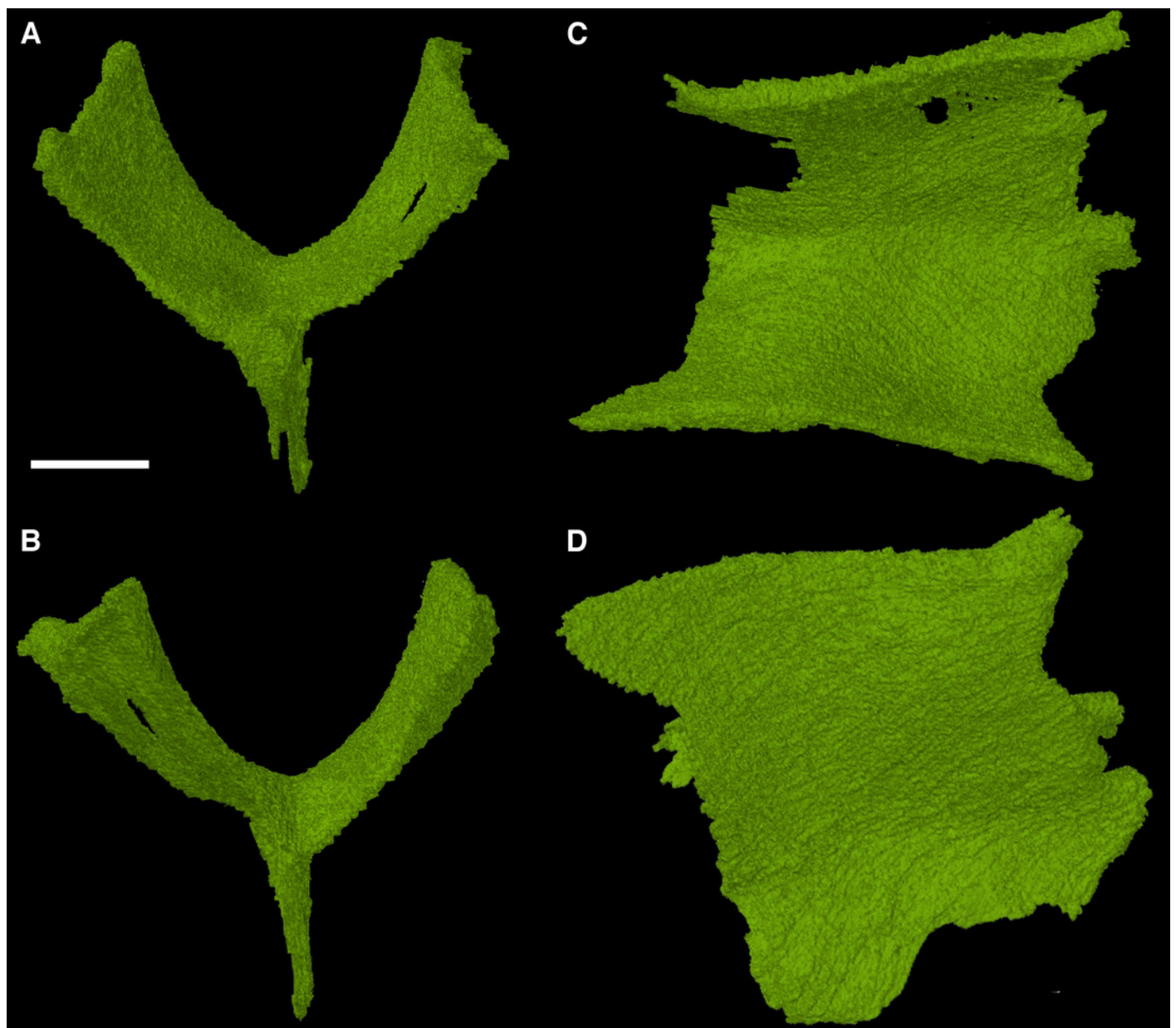
Figure 6

The left epipterygoid of *Feeserpeton oklahomensis*, OMNH 73541, reconstructed from CT data.

A, lateral view, **B**, medial view, **C**, dorsal view, and **D**, ventral view. Scale bar equals 1 mm.
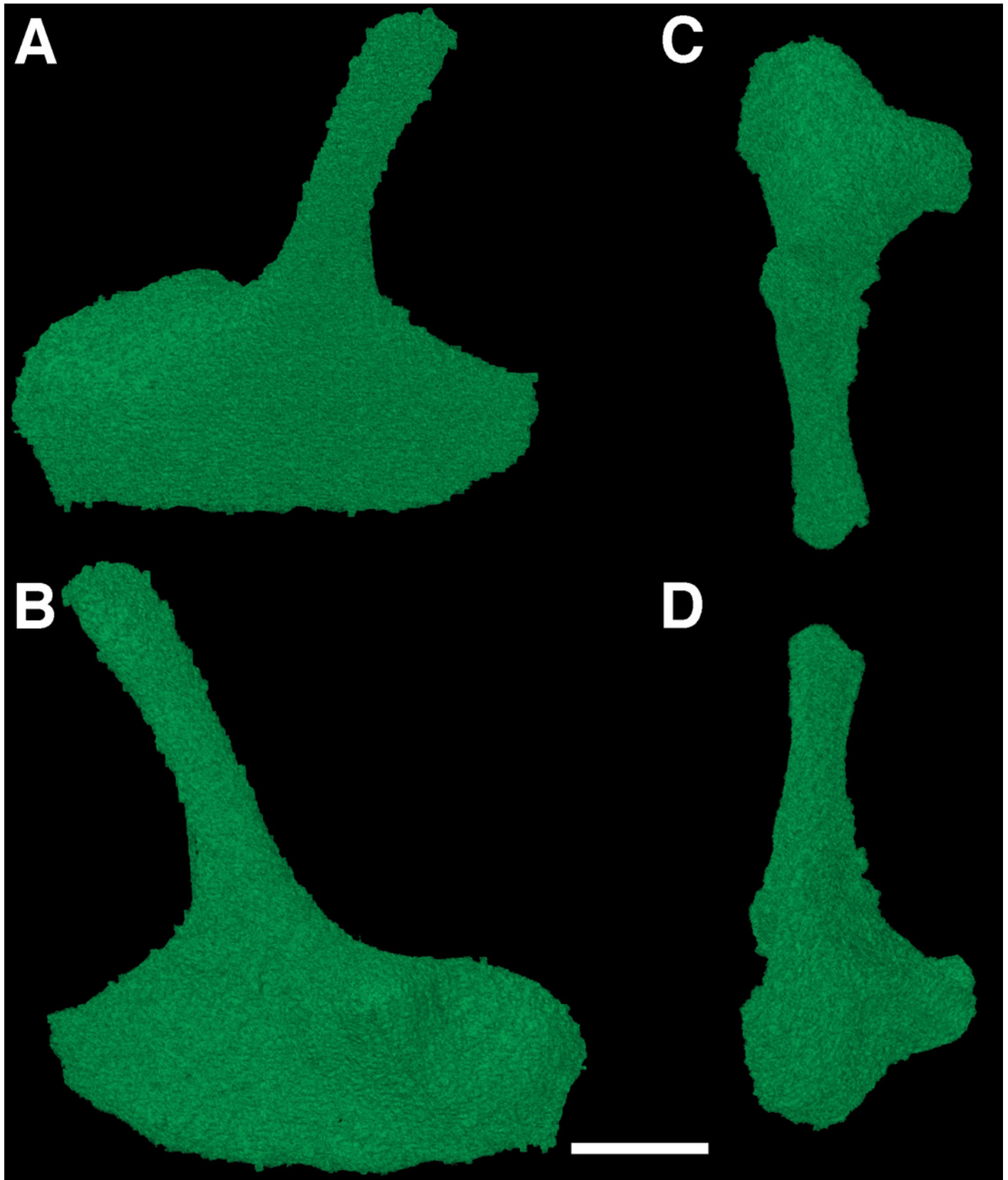
Figure 7

The braincase of *Feeserpeton oklahomensis*, OMNH 73541, reconstructed from CT data.

A, dorsal view, **B**, ventral view, **C**, right lateral view, and **D**, posterior view. Abbreviations: **bo**, basioccipital; **eo**, exoccipitals; **op**, opisthotic; **pro**, prootic;**ps**, parasphenoid; **so**, supraoccipital**st**, stapes; **?**, unknown fragment that may be part of the left stapes or the left opisthotic. Scale bar equals 2 mm.
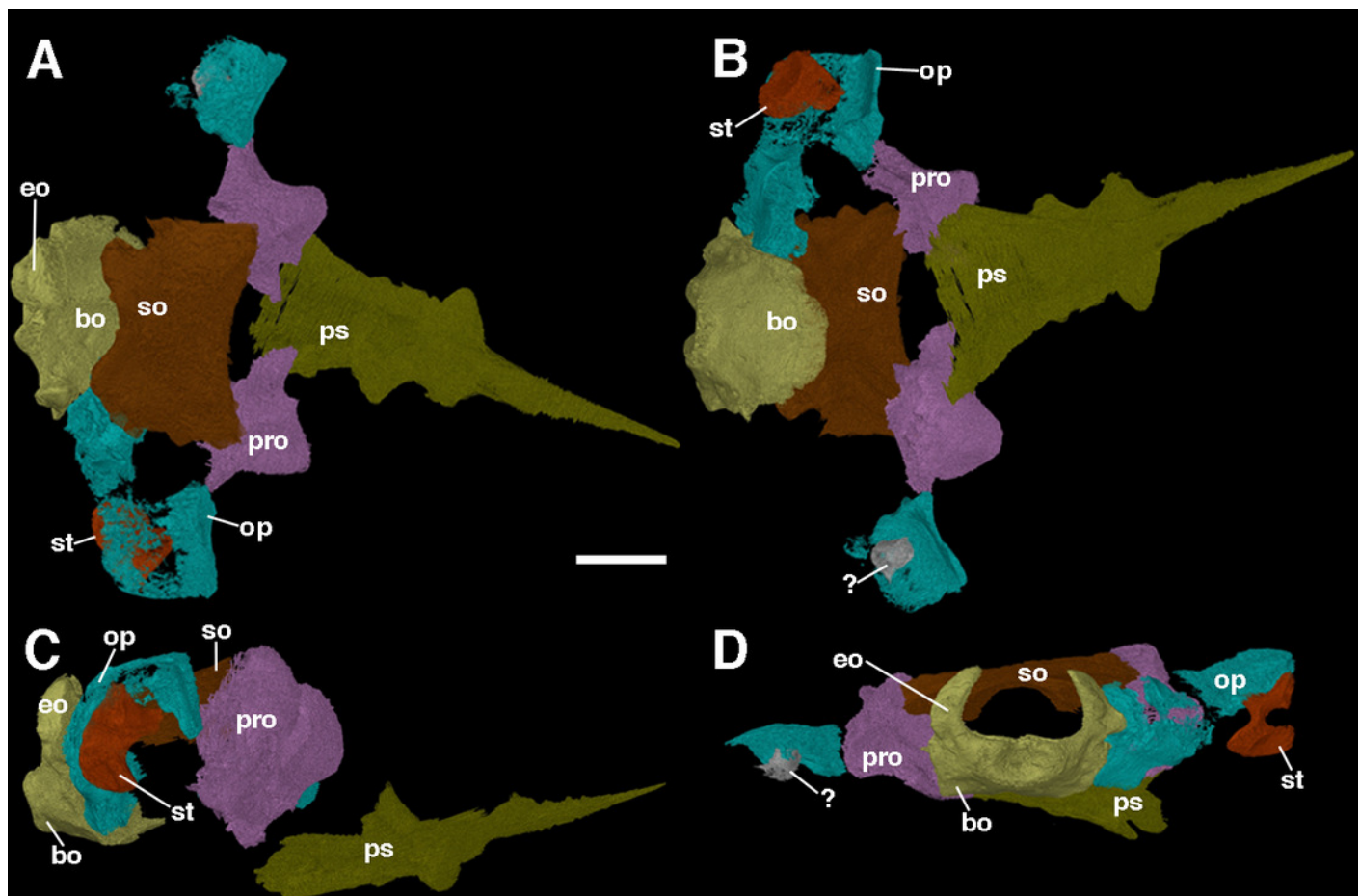
Figure 8

Strict consensus tree obtained from the phylogenetic analysis.

Tree length =667, consistency index = 0.301, rescaled consistency index = 0.195, retention index = 0.647. Nodes of clades of interest are labeled: **A**, Amniota; **B**, Reptilia; **C**, Parareptilia; **D**, Eureptilia; **E**, Lanthanosuchoidea; **F**, Bolosauria; **G**, Nyctiphruretidae; **H**, Nycteroleteridae; **I**, Pareiasauridae; **J**, Procolophonoidea. Bootstrap support values are found above nodes, if no value is indicated it was less than 50%. Bremer support values are found below nodes, if no value is indicated the clade collapsed with the addition of one extra step.